

Entropy production and Fluctuation Relation in turbulent thermal convection

FRANCESCO ZONTA^{1,2} and SERGIO CHIBBARO³

¹ *Department of Electrical, Management and Mechanical Engineering, University of Udine - 33100, Udine, Italy*

² *Institute of Fluid Mechanics and Heat Transfer, Technische Universität Wien - 1060 Wien, Austria*

³ *Sorbonne Universités, UPMC Univ Paris 06, CNRS, UMR 7190, Institut Jean Le Rond d'Alembert F-75005 Paris, France*

received 9 February 2016; accepted in final form 15 June 2016
published online 8 July 2016

PACS 05.20.Jj – Statistical mechanics of classical fluids
PACS 05.40.-a – Fluctuation phenomena, random processes, noise, and Brownian motion
PACS 47.27.-i – Turbulent flows

Abstract – We report on a numerical experiment performed to analyze fluctuations of the entropy production in turbulent thermal convection, a physical configuration taken here as a prototype of an out-of-equilibrium dissipative system. We estimate the entropy production from instantaneous measurements of the local temperature and velocity fields sampled along the trajectory of a large number of pointwise Lagrangian tracers. The entropy production is characterized by large fluctuations and becomes often negative. This represents a sort of “finite-time” violation of the second principle of thermodynamics, since the direction of the energy flux is opposite to that prescribed by the external gradient. We clearly show that the entropy production normalized by a suitable small-scale energy verifies the Fluctuation Relation (FR), even though the system is time-irreversible.

Copyright © EPLA, 2016

Introduction. – Fluctuations of physical systems close to equilibrium are well described by the classical linear-response theory [1,2] that leads to the fluctuation-dissipation relation. The current knowledge of the dynamics of systems far away from equilibrium is instead much more limited, because of the lack of unifying principles. The introduction of the so-called Fluctuation Relation (FR) [3–6] has therefore represented a remarkable result in this area of physics. The FR for nonequilibrium fluctuations reduces to the Green-Kubo and Onsager relations close to equilibrium [7–10] and represents one of the few exact results for systems kept far from equilibrium.

We recall that the FR concerns the symmetry of a representative observable, which is typically linked to the work done on the system, and, through dissipation, to irreversibility. For a Markov process, whose dynamics is described by $\dot{\mathbf{x}}(t) = \mathbf{u}(\mathbf{x}(t), t)$, the representative observable can be written as [11]

$$\beta W_t = \frac{1}{t} \log \frac{\Pi(\{\mathbf{x}(s)\}_0^t)}{\Pi(\{I\mathbf{x}(s)\}_0^t)}, \quad (1)$$

where $\{\mathbf{x}(s)\}_0^t$ and $\{I\mathbf{x}(s)\}_0^t$ are the direct and the time-reversed trajectories in the time interval $[0, t]$, respectively,

while Π indicates probability and β is a suitable energy scale of the system. When FR applies,

$$\log \frac{\Pi(\beta W_t = p)}{\Pi(\beta W_t = -p)} = tp, \quad (2)$$

and W_t is usually called *entropy production rate*. Despite these results, a general response theory for nonequilibrium systems is still to be produced. This suggests that new analyses are required to investigate the behavior of nonequilibrium fluctuations, in particular for macroscopic chaotic systems [12,13].

Turbulence represents the archetype of a macroscopic dynamical system characterized by a large number of degrees of freedom and by strong fluctuations. Moreover, for its intrinsic chaotic nature, turbulence appears as a paradigmatic case to which FR applies, *cum grano salis* [14]. If positively verified, this would strengthen the link between turbulence and nonequilibrium statistical mechanics. In particular, this would justify the hypothesis that a general response theory can be applied also to deterministic time-irreversible systems, at least with the purpose of computing their statistical properties. Given the theoretical and practical importance of these issues,

FR in turbulent flows has been already investigated in the past [15–22]. However, a satisfying statistical description of entropy fluctuations in turbulence is still to be obtained, essentially because of the technical problems associated to the experimental measurement of fluctuations in chaotic systems [23], and also for the difficulty in performing accurate numerical simulations. Note that the choice of a representative observable is the central issue while discussing FR in macroscopic systems [13].

In this work we focus on turbulent Rayleigh-Bénard convection to address the following issues: i) the choice of a representative observable to compute entropy fluctuations; ii) the presence of large deviations of this quantity beyond the linear regime; iii) the applicability of the FR to turbulent thermal convection. To do this, we run Direct Numerical Simulations (DNS) of turbulent Rayleigh-Bénard convection inside a vertically confined fluid layer and we track the dynamics of pointwise tracers, which we use here as probes to measure the local thermodynamic quantities of the system. The fundamental idea of our approach is that turbulence shares similarities with the microscopic nature of heat flows, and turbulence fluctuations correspond to thermal fluctuations [24]. With this in mind, we have chosen a configuration similar to that studied in stochastic thermodynamics [25], which consists of a system kept in contact with two thermostats at different temperatures and characterized by a fluctuating energy flow. A key ingredient in our study is the use of a Lagrangian point of view, which is specifically suited to study the global transport properties of the flow [26]. We will show that entropy production can be evaluated by looking at the work done by buoyancy on moving fluid particles. Provided that the correlations of the measured quantities decay fast enough, we show that the finite-time entropy production exhibits large fluctuations (being often negative) and fulfills FR. Our results complement recent works on granular matter, a simpler but complete model used to describe macroscopic irreversible systems. For granular matter, theory and numerical simulations agree in verifying FR, but only if the correct fluctuating entropy production and temperature are defined [27–29].

Physical problem and modeling. – We consider a turbulent Rayleigh-Bénard convection, in which a horizontal fluid layer is heated from below. Horizontal and wall-normal coordinates are indicated by x_1 , x_2 and x_3 , respectively. Using the Boussinesq approximation, the system is described by the following dimensionless balance equations:

$$\frac{\partial u_i}{\partial x_i} = 0, \quad (3)$$

$$\frac{\partial u_i}{\partial t} + u_j \frac{\partial u_i}{\partial x_j} = -\frac{\partial P}{\partial x_i} + 4\sqrt{\frac{Pr}{Ra}} \frac{\partial^2 u_i}{\partial x_j^2} - \delta_{i,3}\theta, \quad (4)$$

$$\frac{\partial \theta}{\partial t} + u_j \frac{\partial \theta}{\partial x_j} = +\frac{4}{\sqrt{PrRa}} \frac{\partial^2 \theta}{\partial x_j^2}, \quad (5)$$

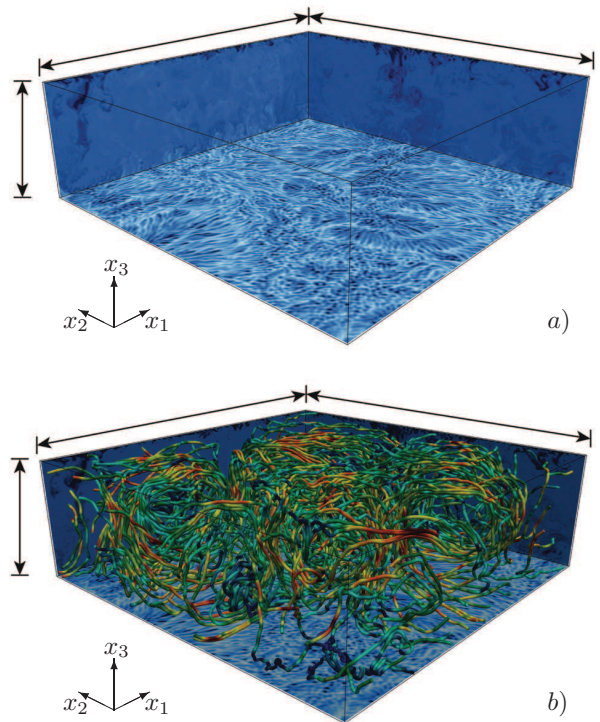


Fig. 1: (Colour online) (a) Two-dimensional contour maps of the temperature distribution computed near the bottom wall and on two vertical slices for Rayleigh-Bénard convection at $Ra = 10^9$. The domain has dimensions $L_{x_1} \times L_{x_2} \times L_{x_3} = 2\pi h \times 2\pi h \times 2h$ and is discretized using $512 \times 512 \times 513$ grid nodes. (b) Example of tracers trajectories for $Ra = 10^9$ colored by the local velocity magnitude.

where u_i is the i -th component of the velocity vector, P is the pressure, $\theta = (T - T_0)/\Delta T$ is the dimensionless temperature, $\Delta T = T_H - T_C$ is the imposed temperature difference between the hot bottom wall (T_H) and top cold wall (T_C), whereas $\delta_{i,3}\theta$ is the driving buoyancy force (acting in the vertical direction x_3 only). The reference velocity is the free-fall velocity $u_{ref} = (g\alpha_0 h \Delta T/2)^{1/2}$, with $h = 0.15$ m the half domain height and g the acceleration due to gravity. The fluid kinematic viscosity ν_0 , thermal diffusivity κ_0 and thermal expansion coefficient α_0 are evaluated at the reference fluid temperature $T_0 = (T_H + T_C)/2 \simeq 29^\circ\text{C}$. The Prandtl and the Rayleigh numbers in eqs. (4), (5) are defined as $Pr = \nu_0/k_0$ and $Ra = (g\alpha_0 \Delta T (2h)^3)/(\nu_0 k_0)$. The size of the domain is $L_{x_1} \times L_{x_2} \times L_{x_3} = 2\pi h \times 2\pi h \times 2h$. Periodicity is imposed on velocity and temperature along the horizontal directions x_1 and x_2 , whereas no slip conditions are enforced for velocity at the top and bottom walls. In our simulations, we keep the Prandtl number $Pr = 4$ and we vary the Rayleigh number between $Ra = 10^7$ and $Ra = 10^9$. An example of the temperature distribution inside our convection cell is given in fig. 1(a). To measure the local values of the field variables, we make use of a Lagrangian approach. The dynamics of $N_p = 1.28 \cdot 10^5$ Lagrangian

Table 1: Summary of the simulations performed with corresponding details of the computation grids. N_{x_1} , N_{x_2} and N_{x_3} correspond to the number of nodes along x_1 , x_2 and x_3 , whereas $\frac{\Delta x_{3,max}}{h}$ and $\frac{\Delta x_{3,min}}{h}$ correspond to the maximum and minimum grid spacings of the (nonuniform) grid along x_3 . The value of the Kolmogorov space/time scales (η_K , τ_K) is also given.

	Simulations		
	\mathcal{S}_1	\mathcal{S}_2	\mathcal{S}_3
Ra	10^7	10^8	10^9
N_{x_1}	128	256	512
N_{x_2}	128	256	512
N_{x_3}	129	257	513
$\frac{\Delta x_1}{h}$	$4.9 \cdot 10^{-2}$	$2.4 \cdot 10^{-2}$	$1.2 \cdot 10^{-2}$
$\frac{\Delta x_2}{h}$	$4.9 \cdot 10^{-2}$	$2.4 \cdot 10^{-2}$	$1.2 \cdot 10^{-2}$
$\frac{\Delta x_{3,max}}{h}$	$2.4 \cdot 10^{-2}$	$1.2 \cdot 10^{-2}$	$6.1 \cdot 10^{-3}$
$\frac{\Delta x_{3,min}}{h}$	$3 \cdot 10^{-4}$	$7.5 \cdot 10^{-5}$	$1.8 \cdot 10^{-5}$
η_K	$1.1 \cdot 10^{-3}$	$5.3 \cdot 10^{-4}$	$2.5 \cdot 10^{-4}$
τ_K	11	2.4	0.5

tracers is computed as

$$\dot{\mathbf{x}}_p = \mathbf{u}(\mathbf{x}_p(t), t) \quad \theta_p = \theta(\mathbf{x}_p(t), t), \quad (6)$$

with $\mathbf{x}_p = (x_{p,1}, x_{p,2}, x_{p,3})$ the tracers position, $\dot{\mathbf{x}}_p = (u_{p,1}, u_{p,2}, u_{p,3})$ their velocity and θ_p their temperature. A visualization of different particle trajectories is shown in fig. 1(b), highlighting also the chaotic nature of the flow.

Equations (4), (5) are discretized using a pseudo-spectral method based on transforming the field variables into wave number space, through Fourier representations for the periodic (homogeneous) directions x_1 and x_2 , and Chebychev representation for the wall-normal (non-homogeneous) direction x_3 . Time advancement is done by a combined Crank-Nicolson scheme for the viscous terms, and an explicit Adams-Bashforth scheme for the nonlinear convective terms. Further details on the numerical method can be found in [30–33]. For the Lagrangian tracking, we have employed 6th-order Lagrangian polynomials to interpolate the fluid velocity and temperature at the tracers position. A 4th-order Runge-Kutta scheme is used for time advancement of the tracers equations (6) [34]. A brief validation of the method is provided in the appendix. An overview of the simulations performed with the corresponding details of the computational grid and the value of the Kolmogorov space/time scales is given in table 1.

Results. – Entropy production for a Markov process is usually defined based on the dynamical probability, a quantity that is generally not accessible in complex systems. To find a representative observable for the system, we start from the balance equation for the turbulent kinetic energy $E_t = 1/2 \langle u'_i u'_i \rangle$, where brackets $\langle \rangle$ indicate statistical average and $u'_i = u_i - \langle u_i \rangle$ velocity fluctuations. For the present flow configuration, $\langle u_i \rangle = 0$. Since the

system is homogeneous along the x_1 and x_2 directions, we obtain

$$\frac{\partial E_t}{\partial t} + \frac{\partial}{\partial x_3} (\langle E_t u'_3 \rangle + \langle u'_3 p' \rangle) = \langle u'_3 \theta' \rangle - \langle \epsilon \rangle, \quad (7)$$

where $\langle \epsilon \rangle = 4 \sqrt{\frac{Pr}{Ra}} \left(\frac{\partial^2 \langle E_t \rangle}{\partial x_3^2} + \left\langle \frac{\partial u'_i}{\partial x_j} \frac{\partial u'_i}{\partial x_j} \right\rangle \right)$ is the turbulent dissipation and $\theta' = \theta - \langle \theta \rangle$ is the temperature fluctuation. The volume-averaged steady-state solution gives $\langle u'_3 \theta' \rangle = \langle \epsilon \rangle$. This provides also an estimate of the entropy production, which from thermodynamics is $\langle \epsilon \rangle / \langle T \rangle$ (with $\langle T \rangle$ the average absolute temperature of the system). We specifically focus on the term $W = \rho_0 g \alpha_0 \theta'_p u'_{3,p}$ measured along the path of the Lagrangian tracers (hence we have $u'_{3,p}$ and θ'_p), which represents the power spent by buoyancy to displace a fluid parcel. Note that W quantifies the vertical flux of energy and is therefore also linked to the vertical Nusselt number [33,35]. Warm fluctuations $\theta'_p > 0$ produce a positive energy flux when associated to positive vertical velocities $u_{p,3} > 0$, whereas cold fluctuations $\theta'_p < 0$ produce a positive energy flux when associated to negative vertical velocity $u_{p,3} < 0$.

We now consider the time-averaged (but fluctuating) expression of the work (per unit volume and time) done by buoyancy on the system,

$$W_\tau = \frac{1}{\tau} \int_0^\tau \mathbf{F}^{ext}(t) \cdot \mathbf{u}(t) dt = \frac{1}{\tau} \int_0^\tau \rho_0 g \alpha_0 \theta'_p u'_{p,3} dt, \quad (8)$$

where \mathbf{F}^{ext} is the external force field due to gravity. This observable is similar to that proposed to analyze the local FR [15]. By contrast, previous experimental studies on macroscopic chaotic systems focused on the behavior of the injected power [16,18,19], which is a measurable quantity that however was found to depart from the predictions given by the FR [27,36]. Although work and heat fluctuations are generally different in stochastic systems [37], we believe that W_τ can give a good estimate of entropy production in turbulent convection.

In the following, we assume that time averages are equivalent to ensemble averages (ergodicity). This assumption is justified if the auto-correlation of W , $R_W = \langle W(t)W(t+\tau) \rangle / \langle W^2 \rangle$, computed after a statistically steady state is reached, exhibits a fast decrease in time [38]. To verify this, we explicitly compute $R_W(\tau)$ for each Ra as a function of the time lag τ . Results are shown in fig. 2. We observe that R_W is characterized by an exponential decay $\exp(-t/\Gamma)$, whose decay rate $1/\Gamma$ increases with increasing Ra . As a consequence, velocity and temperature fluctuations decorrelate faster for large Ra , due to the larger fluctuations observed for increasing Ra . From the behavior of the correlation function R_W , we are able to compute the integral correlation time $\tau_C = \int_0^\infty R_W(\tau) d\tau$. Upon rescaling of the time lag τ by τ_C , the correlation functions R_W computed at different Ra collapse (inset of fig. 2). For $\tau/\tau_C > 1$ the value of the correlation is already $R_W < 0.2$, indicating that from $\tau \simeq \tau_C$

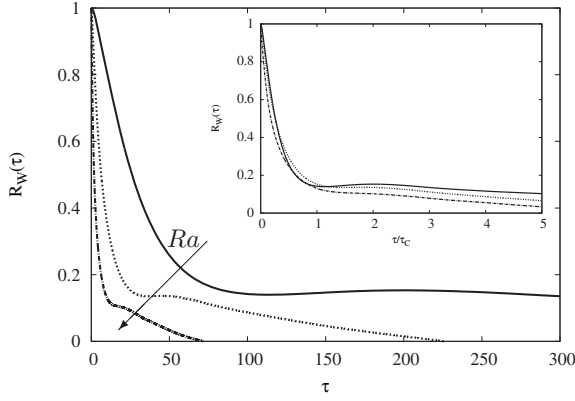


Fig. 2: Lagrangian correlation R_W as a function of the time lag τ for the three different Rayleigh numbers. The collapse of the correlation function upon rescaling of the time lag τ by the integral time scale τ_C is explicitly shown in the inset. Note that $\tau_C = 100$ s for $Ra = 10^7$, $\tau_C = 25$ s for $Ra = 10^8$ and $\tau_C = 7$ s for $Ra = 10^9$.

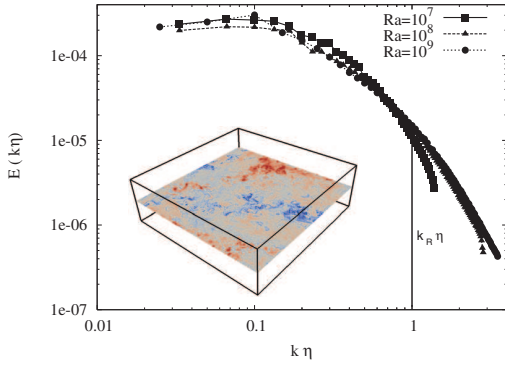


Fig. 3: (Colour online) Time-averaged energy spectra of the turbulent kinetic energy, computed at the center of the channel (on the central plane explicitly shown in the inset) to avoid anisotropy effects due to the nonhomogeneity along the vertical direction. The representative energy scale of the system $\beta^{-1} = (k_B T)_{turb} = 1/2\rho \int_{k>k_R} E(k)dk$, computed assuming $k_R\eta = 1$, gives $\beta = 0.49$ for $Ra = 10^7$, $\beta = 0.33$ for $Ra = 10^8$ and $\beta = 0.3$ for $Ra = 10^9$.

the signal is only barely reminiscent of the initial conditions. This means that τ_C is a representative time scale of the system and suggests that FR can be conveniently tested for $\tau/\tau_C > 1$.

As already discussed, one of the crucial aspects to compute the FR is the choice of the representative energy scale (β) of the system. This energy scale cannot be the thermal energy $k_B T$ [22], with k_B the Boltzmann constant and T the absolute temperature. The main reason is that entropy fluctuations in turbulence are determined by small scale mixing rather than by molecular agitation. Therefore an *effective temperature* must be introduced, as successfully shown for other systems [27,39]. In turbulent flows, following the Kolmogorov cascade picture, we study the

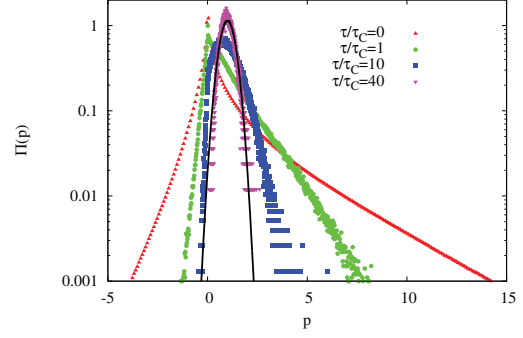


Fig. 4: (Colour online) Probability density function Π of the normalized energy flux $p = W_\tau / \langle W_\tau \rangle$ for $Ra = 10^9$ and for different values of the averaging time window τ/τ_C . The behavior of a Gaussian distribution is explicitly indicated by the solid line. Results from simulations at $Ra = 10^7$ and $Ra = 10^8$ are not shown here because they are qualitatively similar to those at $Ra = 10^9$ and do not add much to the discussion.

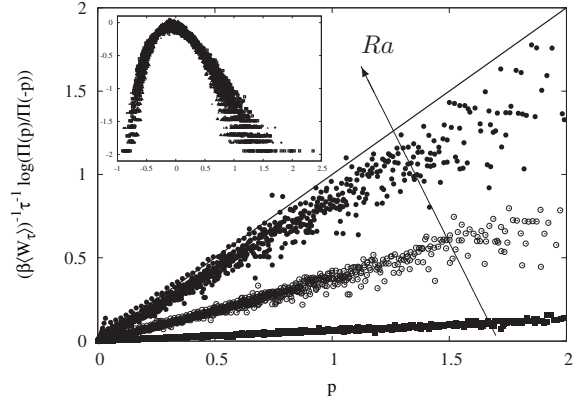


Fig. 5: Behavior of $(\beta \langle W_\tau \rangle)^{-1} \tau^{-1} \log(\Pi(p)/\Pi(-p))$ as a function of p for $1 < \tau/\tau_C < 30$, *i.e.* when the probability density function is not Gaussian. Results are shown for each value of the Rayleigh number Ra (as indicated by the arrow). The solid line represents the theoretical prediction given by the FR, a linear function with slope equal to unity. In the inset, the collapse of the rescaled probability distributions of W_τ at large times onto the large-deviation function is shown (for $5 < \tau < 25$).

nature of entropy fluctuations assuming that β^{-1} is the energy (per unit volume) of the dissipative scales [5,40,41] $\beta^{-1} = (k_B T)_{turb} = 1/2\rho \int_{k>k_R} E(k)dk$, with k_R the wave number characterizing dissipation (*i.e.* $k_R\eta \simeq 1$, with η the Kolmogorov length scale). Following this approach, the value of β is obtained directly from the turbulent kinetic-energy spectrum $E(k)$ (with dimensions m^2/s^2), as shown in fig. 3.

Starting from the Lagrangian measurements of W , we compute the probability density function Π of the normalized flux $p = \frac{W_\tau}{\langle W_\tau \rangle}$, for different values of τ , as shown in fig. 4. For $\tau/\tau_C = 0$, $\Pi(p)$ is highly asymmetric, with the most probable value occurring for $p = 0$ and with positive fluctuations being larger than negative ones. The

asymmetry of $\Pi(p)$ persists also for increasing τ/τ_C and disappears only when the average is done on a large time window ($\tau/\tau_C \geq 40$). In particular, for $\tau/\tau_C \simeq 40$ the distribution peaks around $p \simeq 1$ and recovers an almost Gaussian distribution (explicitly shown by the solid line in fig. 4). Note that at this stage ($\tau/\tau_C \geq 40$), the probability of negative events becomes essentially zero. Altogether these observations suggest that, although the imposed mean temperature difference between the walls induces a net positive vertical energy flux (*i.e.* $\langle W \rangle > 0$), W can often be negative. The occurrence of countergredient fluxes of global transport properties (such as the Nusselt number) is an extremely important phenomenon that has been also observed in other situations [42]. From a physical point of view, small positive and negative values of W are produced by turbulence, which is uncorrelated with the temperature field. These small positive and negative values of W balance each others and do not contribute to the average heat transport [22]. Only large velocity and temperature fluctuations produced by thermal plumes (rising hot plumes and falling cold plumes) are correlated and contribute to the positive mean heat flux.

Based on these observations, it is reasonable to expect that the fluctuations of p are governed by a *large deviation* law $\Pi(p) \sim e^{\tau\zeta(p)}$, with ζ concave. Then, from the behavior of $\Pi(p)$, we measure the quantity

$$\zeta(p) - \zeta(-p) = \sigma(p) = \frac{1}{\tau} \log \frac{\Pi(p)}{\Pi(-p)} \quad (9)$$

for different averaging time τ/τ_C taken in the range $1 < \tau/\tau_C < 30$. The resulting behavior, given in fig. 5, nicely shows that $\sigma(p)$ is a linear function of p ,

$$\sigma(p) = \gamma p. \quad (10)$$

In particular, we observe that the slope γ of the curve increases with increasing Ra and tends (for $Ra = 10^9$) to $\gamma = \beta\langle W_\tau \rangle$. This indicates that the FR introduced in eq. (2) is verified at large times, within numerical and statistical errors. We finally show (inset of fig. 5) the collapse of $\zeta(p) \sim \log \Pi(W_\tau)/\tau$ onto the large-deviation function for $5 < \tau < 25$. The Cramér function $\zeta(p)$, rescaled using its standard deviation σ_τ and its slope C_τ as suggested by [43], collapses for the different values of the averaging time τ shown here (for $5 < \tau < 25$).

Conclusion. – In this letter, we have analyzed the behavior of entropy fluctuations in turbulent thermal convection, taken here as a paradigmatic case of a complex out-of-equilibrium system. We have performed Direct Numerical Simulations of a turbulent Rayleigh-Bénard flow inside a vertically confined fluid layer and we have followed the dynamics of pointwise Lagrangian tracers to measure the local quantities of the flow. We have shown that entropy production can be evaluated by looking at the work done by buoyancy on fluid particles, $W_\tau \propto \theta'_p u'_{3,p}$. We have found that W_τ is often negative, and is characterized by fluctuations that follow the FR beyond the

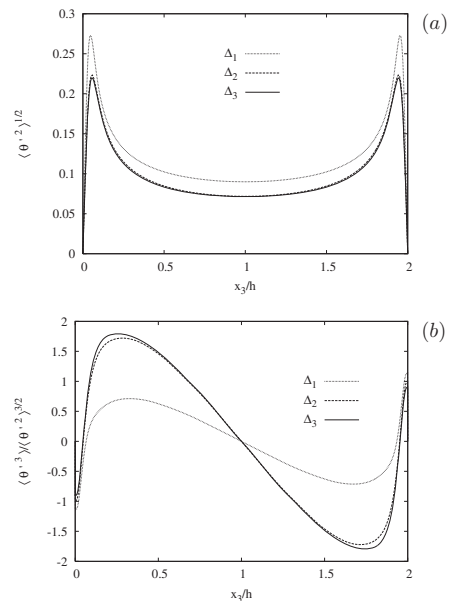


Fig. 6: Grid convergence analysis: wall-normal behavior of the root mean square $\langle \theta'^2 \rangle^{1/2}$ (panel (a)) and of the skewness factor $\langle \theta'^3 \rangle / \langle \theta'^2 \rangle^{3/2}$ (panel (b)) of temperature fluctuations. Results are obtained from simulations at Rayleigh number $Ra = 10^7$ and using three different grids : grid Δ_1 has $64 \times 64 \times 65$ nodes; grid Δ_2 has $128 \times 128 \times 129$ nodes; grid Δ_3 has $256 \times 256 \times 257$ nodes in the streamwise (x_1), spanwise (x_2) and wall-normal (x_3) direction, respectively.

linear regime, provided that a representative *effective temperature* is employed. Here we defined the effective temperature as the kinetic energy of the small scales, which can be taken as a sort of temperature. However, this is a crucial point that deserves further investigation, since other physical quantities (for instance the energy dissipation rate ϵ) can be used for this scope as well [44].

Present results shed new light on turbulence, allowing an *a priori* estimate of the behavior of fluctuations of energy flux or entropy production and giving access to the Cramér function. New simulations in different configurations and at higher Reynolds/Rayleigh numbers are foreseen to assess the robustness of present results.

We thank MASSIMO CENCINI, ANDREA CRISANTI, ANDREA PUGLISI, LAMBERTO RONDONI, DARIO VILLAMAINA and ANGELO VULPIANI for fruitful discussions.

APPENDIX

For validation purposes, in fig. 6 we show the wall-normal behavior (as a function of x_3/h) of the root mean square $\langle \theta'^2 \rangle^{1/2}$ (fig. 6(a)) and of the skewness factor $\langle \theta'^3 \rangle / \langle \theta'^2 \rangle^{3/2}$ (fig. 6(b)) of temperature fluctuations for $Ra = 10^7$. Results are compared using three different grid resolutions Δ_1 ($64 \times 64 \times 65$ nodes), Δ_2 ($128 \times 128 \times 129$ nodes) and Δ_3 ($256 \times 256 \times 257$ nodes). Note

that the computational grids have a nonuniform spacing (with near-wall refinement) along the wall-normal coordinate x_3 , due to the adoption of Chebychev polynomials ($T_{n_3}(x_3) = \cos(n_3 \cos^{-1}(x_3/h))$ is the Chebychev polynomial of order n_3 along x_3). Results in fig. 6(a), (b) indicate that the computational grid Δ_2 is accurate enough to properly resolve all the flow scales at $Ra = 10^7$, and further grid refinement is not required (the difference with a finer grid, Δ_3 , is always below 3% for both second- and third-order moments). Increasing Ra , temperature and velocity flow structures become smaller and the computational grid must be refined accordingly (see table 1). The grid resolutions employed here are consistent with those found in the literature [45].

REFERENCES

- [1] ONSAGER L., *Phys. Rev.*, **37** (1931) 405; **38** (1931) 2265; KUBO R., *J. Phys. Soc. Jpn.*, **12** (1957) 570.
- [2] MARCONI U. M. B., PUGLISI A., RONDONI L. and VULPIANI A., *Phys. Rep.*, **461** (2008) 111.
- [3] EVANS D. J., COHEN E. and MORRISS G., *Phys. Rev. Lett.*, **71** (1993) 2401.
- [4] EVANS D. J. and SEARLES D. J., *Phys. Rev. E*, **50** (1994) 1645.
- [5] GALLAVOTTI G. and COHEN E., *Phys. Rev. Lett.*, **74** (1995) 2694; *J. Stat. Phys.*, **80** (1995) 931.
- [6] JARZYNSKI C., *Phys. Rev. Lett.*, **78** (1997) 2690.
- [7] GALLAVOTTI G., *Phys. Rev. Lett.*, **77** (1996) 4334.
- [8] SEARLES D. J., RONDONI L. and EVANS D. J., *J. Stat. Phys.*, **128** (2007) 1337.
- [9] CHETRIT R. and GAWEDZKI K., *Commun. Math. Phys.*, **282** (2008) 469.
- [10] GALLAVOTTI G., *Nonequilibrium and Irreversibility* (Springer) 2014.
- [11] LEBOWITZ J. and SPOHN H., *J. Stat. Phys.*, **29** (1982) 39.
- [12] RITORT F., *Work Fluctuations, Transient Violations of The Second Law and Free-Energy Recovery Methods: Perspectives in Theory and Experiments*, in *Proceedings of the Poincaré Seminar 2003* (Springer) 2004, pp. 193–226.
- [13] CILIBERTO S., GOMEZ-SOLANO R. and PETROSYAN A., *Annu. Rev. Condens. Matter Phys.*, **4** (2013) 235.
- [14] GALLAVOTTI G. and LUCARINI V., *J. Stat. Phys.*, **156** (2014) 1027.
- [15] CILIBERTO S. and LAROCHE C., *J. Phys. IV*, **8** (1998) 215.
- [16] CILIBERTO S., GARNIER N., HERNANDEZ S., LACPATIA C., PINTON J.-F. and CHAVARRIA G. R., *Physica A: Stat. Mech. Appl.*, **340** (2004) 240.
- [17] SCHUMACHER J. and ECKHARDT B., *Physica D: Nonlinear Phenom.*, **187** (2004) 370.
- [18] FALCON E., AUMAÎTRE S., FALCÓN C., LAROCHE C. and FAUVE S., *Phys. Rev. Lett.*, **100** (2008) 064503.
- [19] CADOT O., BOUDAUD A. and TOUZÉ C., *Eur. Phys. J. B*, **66** (2008) 399.
- [20] BIFERALE L., PIEROTTI D. and VULPIANI A., *J. Phys. A: Math. Gen.*, **31** (1998) 21.
- [21] GALLAVOTTI G., RONDONI L. and SEGRE E., *Physica D: Nonlinear Phenom.*, **187** (2004) 338.
- [22] SHANG X.-D., TONG P. and XIA K.-Q., *Phys. Rev. E*, **72** (2005) 015301.
- [23] ZAMPONI F., *J. Stat. Mech.: Theory Exp.* (2007) P02008.
- [24] RUELLE D. P., *Proc. Natl. Acad. Sci. U.S.A.*, **109** (2012) 20344.
- [25] SEKIMOTO K., *Stochastic Energetics*, Vol. **799** (Springer) 2010.
- [26] TOSCHI F. and BODENSCHATZ E., *Annu. Rev. Fluid Mech.*, **41** (2009) 375.
- [27] PUGLISI A., VISCO P., BARRAT A., TRIZAC E. and VAN WIJLAND F., *Phys. Rev. Lett.*, **95** (2005) 110202.
- [28] PUGLISI A. and VILLAMAINA D., *EPL*, **88** (2009) 30004.
- [29] SARRACINO A., VILLAMAINA D., GRADENIGO G. and PUGLISI A., *EPL*, **92** (2010) 34001.
- [30] ZONTA F., ONORATO M. and SOLDATI A., *J. Fluid Mech.*, **697** (2012) 175.
- [31] ZONTA F., *Int. J. Heat Fluid Flow*, **44** (2013) 489.
- [32] ZONTA F. and SOLDATI A., *J. Heat Transfer*, **136** (2014) 022501.
- [33] LIOT O., SEYCHELLES F., ZONTA F., CHIBBARO S., COUDARCHET T., GASTEUIL Y., PINTON J., SALORT J. and CHILLÁ F., *J. Fluid Mech.*, **794** (2016).
- [34] ZONTA F., MARCHIOLI C. and SOLDATI A., *Acta Mech.*, **195** (2008) 305.
- [35] GASTEUIL Y., SHEW W., GIBERT M., CHILLA' F., CASTAING B. and PINTON J., *Phys. Rev. Lett.*, **99** (2007).
- [36] FARAGO J., *J. Stat. Phys.*, **107** (2002) 781.
- [37] VAN ZON R. and COHEN E., *Phys. Rev. E*, **69** (2004) 056121.
- [38] MONIN A. S. and YAGLOM A. M., *Statistical Fluid Mechanics: Mechanics of Turbulence* (Dover) 2007.
- [39] CUGLIANDOLO L. F., KÜRCHAN J. and PELITI L., *Phys. Rev. E*, **55** (1997) 3898.
- [40] GALLAVOTTI G., *Physica D: Nonlinear Phenom.*, **105** (1997) 163.
- [41] RONDONI L. and SEGRE E., *Nonlinearity*, **12** (1999) 1471.
- [42] HUISMAN S., VAN GILS D., GROSSMANN S., SUN C. and LOHSE D., *Phys. Rev. Lett.*, **108** (2012).
- [43] RONDONI L. and MORRISS G. P., *Open Syst. Inf. Dyn.*, **10** (2003) 105.
- [44] XU H., PUMIR A., FALKOVICH G., BODENSCHATZ E., SHATS M., XIA H., FRANCOIS N. and BOFFETTA G., *Proc. Natl. Acad. Sci. U.S.A.*, **111** (2014) 7558.
- [45] STEVENS R. J. A. M., VERZICCO R. and LOHSE D., *J. Fluid Mech.*, **643** (2010) 495.